

Study of organic thin film transistor with polymethylmethacrylate as a dielectric layer

Tsung-Syun Huang,^{a)} Yan-Kuin Su,^{b)} and Po-Cheng Wang

Advanced Optoelectronic Technology Center, Institute of Microelectronics, Department of Electrical Engineering, National Cheng Kung University, Tainan 701, Taiwan

(Received 28 June 2007; accepted 2 August 2007; published online 27 August 2007)

The properties of pentacene-based organic thin film transistors (OTFTs) with polymethylmethacrylate (PMMA) as a dielectric layer have been investigated. The concentration of PMMA was about 8 wt % with toluene as solvent. The pentacene film on PMMA dielectric layer displays high thin film quality according to results of x-ray diffraction scan and atomic force microscopy. The crystalline size was about 33.96 nm and the grain size was about 1000–1500 nm. The pentacene-based OTFTs with PMMA as a dielectric layer exhibited excellent electric characteristics, including a high mobility of 0.241 cm²/V s or larger, an on/off current ratio of 10⁴ or larger, and the threshold voltage of less than –6.3 V. © 2007 American Institute of Physics.

[DOI: 10.1063/1.2775333]

Organic materials were generally used in many electronic devices such as light emitting diodes,¹ thin film transistors,^{2,3} and photodetectors.⁴ Due to varieties of materials and fabrication methods used in making organic electron devices and due to their other amazing characteristics, many researchers are attracted to jump into this field. For organic thin film transistors, many different materials, structures, and special modification methods were used to improve the characteristics of devices. Nowadays, the performance characteristics of organic thin film transistors (OTFTs) were almost the same as amorphous silicon (*a*-Si) which was commonly adopted in the modern liquid crystal display. Pentacene-based OTFTs with a field-effect mobility greater than 1 cm²/V s and an on/off current ratio over 10⁸ have been demonstrated by several groups.^{5–7}

Surface properties of a dielectric layer, i.e., surface energy (γ_s),⁸ crystallite size, grain size, and surface roughness (R_{rms}), were the distinctive factors that determine potential improvements in electric characteristics of OTFTs. Polymeric insulators have been considered as preferable gate dielectric materials due to their numerous advantages over inorganic materials: i.e., flexible, hydrophilic, easy process, and low cost. Hence, in addition to studying surface properties, it is also interesting to explore the influence of polar groups of polymer insulators on the structures of organic semiconductors and the corresponding performance of OTFTs.

In this letter, polymethylmethacrylate (PMMA) was used as a dielectric layer to substitute SiO₂ in order to confer the transfer characteristics of OTFTs with PMMA as a dielectric layer. We studied the quality of pentacene thin film on PMMA by atomic force microscopy (AFM) and x-ray diffraction (XRD). Comparison was made with other OTFTs fabricated with SiO₂ as a dielectric layer. The resultant surface free energy between pentacene and insulator was also deduced.

The PMMA-insulator OTFT structure was shown in Fig. 1. The OTFTs were fabricated on highly doped *n*-type silicon

substrates. PMMA (molecular weight=996 000) was dissolved in toluene with a concentration of 8 wt % and then spin coated onto the highly doped *n*-type silicon substrate to form a 300-nm-thick thin film, which serve as polymer insulator. The PMMA layer was baked for 1 h at the temperature of 100 °C. For comparison, SiO₂ was thermally grown on the highly doped *n*-type silicon substrate with the thickness of SiO₂ kept also at 300 nm. The molecular structures of PMMA and pentacene were also shown in Fig. 1. Pentacene thin films were grown onto SiO₂ and PMMA by vacuum evaporation method with a thickness of 60 nm each. The deposition rate of approximately 0.5 Å/s and a base pressure of approximately 5 × 10⁻⁶ torr were applied. After depositing pentacene thin film, a 200-nm-thick Au layer was deposited through a shadow mask to, respectively, pattern the drain, source, and gate electrodes using a thermal evaporator. The channel length and width of these devices were 50 and 1000 μm, respectively. The pentacene film was studied by XRD in the symmetric reflection coupled θ -2 θ arrangement. XRD patterns were obtained using Cu K α radiation ($\lambda_{K\alpha 1}$ = 1.5406 Å) and a wide-angle graphite monochromator. The grain size and R_{rms} (roughness) were measured by AFM. For the surface free energy, the contact angles (face contact-angle meter, Kyowa Kaimenkagaku Co.) of two test liquids were measured. The measurement was conducted by placing water and di-iodomethane of two test liquids on the surfaces of PMMA and SiO₂. Electrical characteristics of OTFTs were measured by a Keithley 4200-SCS system.

The morphology and the structural properties of pentacene were shown in Figs. 2 and 3. Figure 2 shows the x-ray diffraction spectra of pentacene thin films deposited onto PMMA and SiO₂, respectively. From this figure, it can be found that the peak intensity of Bragg reflection of pentacene thin film on PMMA was more conspicuous than that on SiO₂. It means that the crystallite quality of pentacene thin film on PMMA was greater than that of pentacene thin film on SiO₂. Both films have two major diffraction peaks, which can be attributed to “thin film phase” (00 l') and “triclinic bulk phase” (00 l), respectively.^{9,10} We observed the same 2 θ of (00 l') peak, indicating a thin film phase with the same interlayer spacing of 15.4 Å, for both pentacene films. The

^{a)}Electronic mail: 17894110@ccmail.ncku.edu.tw

^{b)}Electronic mail: yksu@mail.ncku.edu.tw

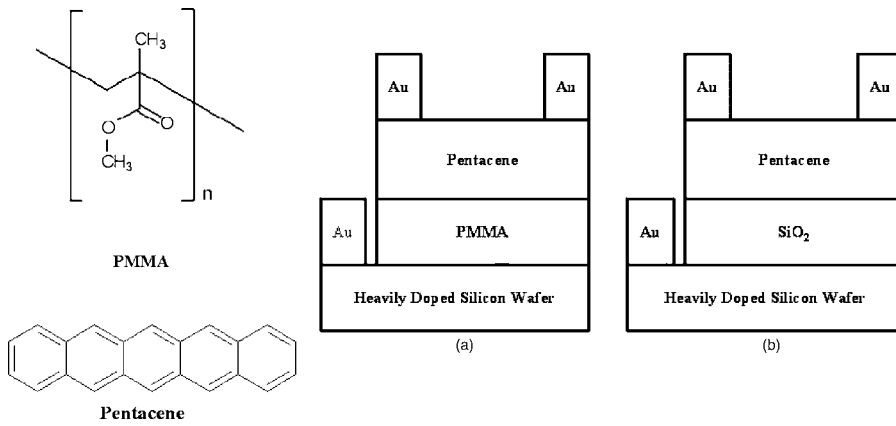


FIG. 1. Schematic of molecular structures of PMMA and pentacene showing alongside with (a) pentacene-base OTFTs with PMMA as a dielectric layer and (b) pentacene-base OTFTs with SiO_2 as a dielectric layer.

minimum crystalline size perpendicular to the $(00l')$ planes was calculated using the paracrystal theory.¹¹ Since the $(00l')$ planes are oriented parallel to the substrate, this calculation provides a measurement of the crystal size and qual-

ity perpendicular to the film plane. The following formula was used:

$$(\delta s)^2 = (\delta s)_c^2 + (\delta s)_{\text{II}}^2 = \frac{1}{\bar{L}_{hkl}^2} + \frac{\pi^4 g_{\text{II}}^4 m^4}{\bar{d}_{hkl}^2}, \quad (1)$$

where

$$\delta s = \frac{2 \cos \theta \delta \theta}{\lambda} \quad (2)$$

was the overall broadening, λ was the x-ray wavelength, θ was the diffraction angle, $\delta \theta$ was expressed in radians, $(\delta s)_c$ was broadening due to crystallite size, $(\delta s)_{\text{II}}$ was broadening due to lattice distortions of the second kind, m was the diffraction order, \bar{d}_{hkl} was the average (hkl) plane spacing, \bar{L}_{hkl} was the average crystalline size perpendicular to the (hkl) planes, and g_{II} was the mean distance fluctuation between successive (hkl) planes due to distortion of the second kind. Our measurements were based on the full widths at half maximum of the diffraction peaks, thus repeating the methodology used in previous reports.^{8,9} The estimated $L_{00l'}$ values of pentacene film grown on PMMA and SiO_2 were equal to 33.96 and 12.8 nm, respectively. XRD analysis shows that pentacene films on PMMA layer have a better crystal quality than that on SiO_2 layer. The grain sizes and morphologies of pentacene films were observed by AFM to assess the crystalline qualities, as shown in Fig. 3. According to Fig. 3, it can be found that the grain size of pentacene deposited onto PMMA layer was 1000–1500 nm and the grain size of pen-

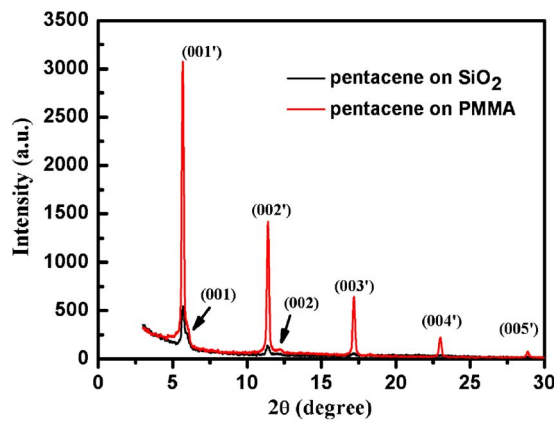


FIG. 2. (Color online) X-ray diffraction spectra of pentacene thin films on PMMA and SiO_2 .

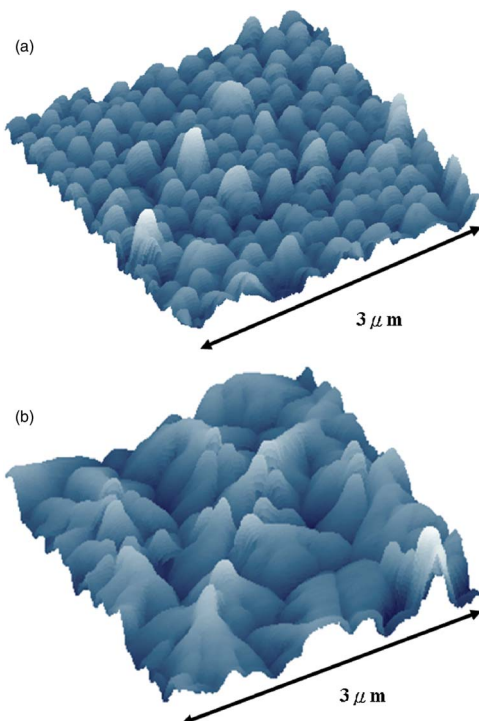


FIG. 3. (Color online) Atomic force microscope images of pentacene thin films on (a) SiO_2 and (b) PMMA.

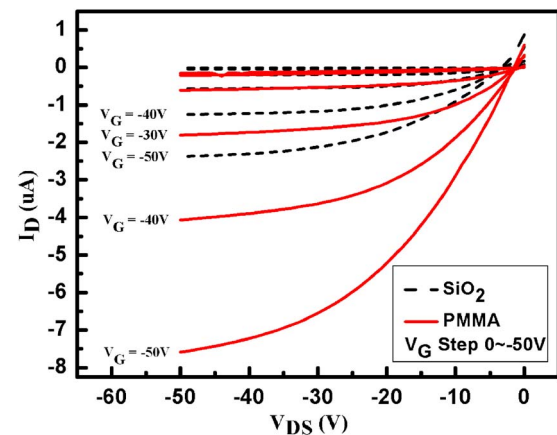


FIG. 4. (Color online) Electrical transfer characteristics of pentacene-based OTFTs with PMMA as a dielectric layer (dotted line) and with SiO_2 as a dielectric layer (solid line) when V_{GS} was increased from 0 to 50 V.

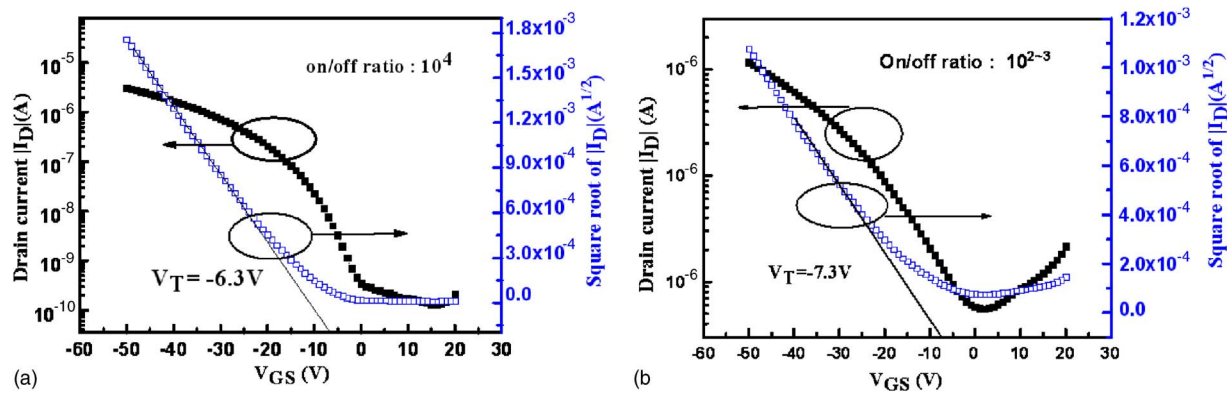


FIG. 5. (Color online) Semilogarithmic plots of both drain current and square root of drain current vs gate voltage showing the transfer characteristics of (a) pentacene OTFT with PMMA as a dielectric layer and (b) pentacene OTFT with SiO₂ as a dielectric layer when V_{DS} was set at -50 V.

TABLE I. Crystalline quality of pentacene films and the corresponding electrical performance of the pentacene-based OTFTs.

Gate dielectric	Device performance			Pentacene film quality		
	V_T (V)	μ_{sat} (cm ² /V s)	On/off current ratio	Crystalline size (Å)	Grain size (nm)	Surface roughness (nm)
PMMA	-6.3	0.241	10 ⁴	339.6	1000–1500	11.376
SiO ₂	-7.3	0.0372	10 ³	128	100–300	12.3

tacene deposited onto SiO₂ layer was 100–300 nm. The R_{rms} (roughness) of pentacene on PMMA layer and SiO₂ were 11.376 and 12.3 nm, respectively. Hence, the pentacene film on the PMMA layer apparently had significantly larger grain size as compared to a similar film on the SiO₂ layer. The quality of pentacene on PMMA layer was better than that of pentacene on SiO₂.

The surface free energy of PMMA and SiO₂ was measured by the contact angle of water and di-iodomethane. The values of surface free energy of PMMA and SiO₂ were 47.5 and 45.6 mJ/m², respectively. The surface free energy of pentacene was 47.4 mJ/m². Obviously, the surface free energy of PMMA matches with that of the pentacene thin film. A matching surface free energy significantly contributes to the enhancement of mobility in OTFTs which results in a decrease in the threshold voltage.⁸

Figure 4 shows the transfer characteristics (I_D - V_{DS}) of the PMMA-insulator pentacene OTFT and SiO₂ insulator pentacene OTFT fabricated on the high doping n -type silicon substrate. From this figure, it can be found that the magnitude of the drain saturation current I_D produced by the OTFT with PMMA-insulator layer was significantly larger than that of a similar OTFT with SiO₂ insulator layer at the same gate voltage V_G . Figures 5(a) and 5(b) present plots of $\log I_D$ and the square root of I_D as a function of V_{GS} for OTFTs with PMMA and SiO₂ insulator layers, respectively, when V_{DS} was set at -50 V. Saturation field-effect mobility μ_{sat} , on/off current ratio, and threshold voltage V_{th} were all measured for OTFTs with the PMMA and SiO₂ insulator layers by a curve fitting applied to the linear region between -20 and -40 V of V_{GS} and the results are listed in Table I.

In conclusion, we have fabricated and characterized the pentacene-based OTFTs with PMMA as a dielectric layer in this letter. This study gave clear experimental evidence that the quality of pentacene grown on the PMMA dielectric layer

was better than that of a similar film grown on SiO₂ dielectric layer. XRD was used to measure the diffraction intensity in order to study the crystalline quality of pentacene thin film on PMMA and SiO₂. We also used AFM to measure the grain size and roughness of pentacene grown on PMMA and SiO₂ and subsequently deduce a match in surface free energy between pentacene and PMMA. The maximum saturation field-effect mobility was above 0.241 cm²/V s. It was also found that the transfer characteristics of OTFT with PMMA dielectric layer were greater than those of OTFT with SiO₂ dielectric layer. Giving the merits of PMMA because of its polymeric nature, for the purpose of fabricating OTFTs on flexible substrates, there is a possibility that SiO₂ can be substituted by PMMA as a dielectric layer. It is foreseeable that the high performance flexible OTFTs will be expected in the future.

¹J. R. Sheats, H. Antoniadis, M. Husechen, W. Leonard, J. Miller, R. Moon, D. Roitman, and A. Stocking, *Science* **273**, 884 (1996).

²C. O. Dimitrikopoulos and D. J. Mascaró, *IBM J. Res. Dev.* **45**, 11 (2001).

³H. Fuchigami, A. Tsumura, and H. Kozuka, *Appl. Phys. Lett.* **63**, 1372 (1993).

⁴P. Peumans and S. R. Forrest, *Appl. Phys. Lett.* **79**, 126 (2001).

⁵Y. Y. Lin, D. J. Gundlach, S. F. Nelson, and T. N. Jackson, *IEEE Electron Device Lett.* **18**, 606 (1997).

⁶M. Shtein, J. Mapel, J. B. Benziger, and S. R. Forrest, *Appl. Phys. Lett.* **81**, 268 (2002).

⁷D. Knipp, R. A. Street, A. Völkel, and J. Ho, *J. Appl. Phys.* **93**, 347 (2003).

⁸W. Y. Chou, C. W. Kuo, H. L. Cheng, and Y. R. Chen, *Appl. Phys. Lett.* **89**, 112126 (2006).

⁹T. Minakata, H. Imai, M. Ozaki, and K. Saco, *J. Appl. Phys.* **72**, 5220 (1996).

¹⁰C. D. Kimitrakopoulos, A. R. Brown, and A. Pomp, *J. Appl. Phys.* **80**, 2501 (1996).

¹¹L. E. Alexander, *X-Ray Diffraction Methods in Polymer Science* (Wiley, New York, 1969), p. 429.